



Published in final edited form as:

Nat Genet. 2009 October ; 41(10): 1144–1149. doi:10.1038/ng.441.

Tissue regenerative delays and synthetic lethality in adult mice upon combined deletion of *ATR* and *p53*

Yaroslava Ruzankina^{*}, David W. Schoppa^{*}, Amma Asare, Carolyn E. Clark, Robert H. Vonderheide, and Eric J. Brown¹

Abramson Family Cancer Research Institute, Department of Cancer Biology, University of Pennsylvania School of Medicine, Philadelphia, PA 19104-6160

Abstract

Trp53 (*p53*) loss of function has previously been shown to rescue tissue maintenance and developmental defects resulting from DNA damage or DNA repair gene mutations^{1–12}. Herein, we report that *p53* deficiency significantly exacerbates tissue degeneration caused by mosaic deletion of the essential genome maintenance regulator *ATR*. Combined loss of *ATR* and *p53* (*p53*^{-/-}*ATR*^{mKO}) led to severe defects in hair follicle regeneration, localized inflammation (Mac1⁺Gr1⁺ infiltrates), accelerated deterioration of the intestinal epithelium, and synthetic lethality in adult mice. Tissue degeneration in *p53*^{-/-}*ATR*^{mKO} mice was characterized by the accumulation of cells maintaining high levels of DNA damage. Moreover, the elevated presence of these damaged cells in both progenitor and downstream compartments in the skin coincided with delayed compensatory tissue renewal from residual *ATR*-expressing cells. Together, our results indicate that combined loss of *ATR* and *p53* in adult mice leads to the accumulation of highly damaged cells, which consequently impose a barrier to regeneration from undamaged progenitors.

Keywords

ATR; *p53*; DNA damage; tissue regeneration; aging; cancer

Tissue development, homeostasis, and renewal are strongly influenced by processes that control the accumulation of damaged, unproductive cells. Through its functions in cell cycle regulation and apoptosis, the *p53* transcription factor plays a central role in these processes,

Users may view, print, copy, download and text and data-mine the content in such documents, for the purposes of academic research, subject always to the full Conditions of use: http://www.nature.com/authors/editorial_policies/license.html#terms

¹To whom correspondence should be addressed: Abramson Family Cancer Research Institute, Department of Cancer Biology, University of Pennsylvania School of Medicine, 514 BRB II/III, 421 Curie Boulevard, Philadelphia, PA 19104-6160, Phone: (215) 746-2805, Fax: (215) 573-2486, brownj@mail.med.upenn.edu.

^{*}These authors contributed equally to this work.

Note: Supplementary information is available on the Nature Genetics website.

AUTHOR CONTRIBUTIONS

Y.R., D.W.S. and E.J.B. designed and interpreted the experiments and wrote the manuscript. Y.R. and D.W.S. performed all of the experiments, with assistance from A.A. (mouse maintenance, qPCR and histological analysis) and C.C. and R.H.V. (quantification of Gr1⁺Mac1⁺ cell infiltration).

COMPETING INTERESTS STATEMENT

The authors declare that they have no competing financial interests.

particularly in response to DNA damage. For example, developmental arrest, tissue homeostatic failures, and premature cellular senescence in numerous mouse models harboring DNA repair gene mutations are partially rescued by *p53* deficiency^{1–12}. Furthermore, *p53* pathway hyperactivation leads to tissue deterioration and promotes the appearance of several age-associated pathologies in mice^{13,14}, arguing that unregulated *p53* engagement can present a significant barrier to tissue renewal. However, mice expressing additional copies of *p53* and *Cdkn2a* (*Arf*) under normal regulatory control (*s-Arf/p53* mice) exhibit enhanced antioxidant gene expression, decreased accumulation of mutated cells, and a significantly extended lifespan¹⁵. This study and others have indicated that augmented *p53* pathway activity can enhance tissue renewal by reducing ROS levels¹⁵ and by limiting the accumulation of damaged cells that impede repopulation from competent progenitors^{15–18}.

Deletion of the *ATR* checkpoint kinase leads to an increase in double strand break formation in the course of normal DNA replication^{19–22} and to the activation of *p53* (Supplementary Fig. 1). Previously, we have demonstrated that such deletion in the presence of wild-type *p53* leads to the rapid elimination of *ATR*-deleted (*ATR*^{-/-}) cells from adult tissues that maintain high rates of cellular proliferation; however, cellularity in most tissues is quickly restored by concomitant regeneration from progenitors that have escaped *ATR* deletion²³. Despite this initial reconstitution, *ATR*-mosaic knockout (*ATR*^{mKO}) mice ultimately fail to maintain tissue homeostasis and exhibit age-related phenotypes²³. In light of the proposed functions for *p53* in tissue homeostasis, *p53* activation in *ATR*^{mKO} mice could drive acute tissue degeneration by reducing cellularity or, alternatively, facilitate immediate regeneration by limiting the accumulation of damaged cells, thus promoting renewal from undamaged progenitors.

To investigate these models, systemic mosaic deletion of *ATR* in *p53*^{+/+} and *p53*^{-/-} mice was performed as described previously²³ by tamoxifen (TAM)-induced acute activation of a ubiquitously expressed form of Cre recombinase (*UBC-Cre-ERT2*). The rates of Cre-mediated lox recombination of the *ATR*^{lox} allele were identical regardless of *p53* status, as demonstrated by equivalent *ATR*^{lox} recombination rates in the brain, bone marrow and intestines of *ATR*^{lox/+} (*ATR*^{het}) mice, and by deletion rates in the brains of *ATR*^{lox/-} (*ATR*^{mKO}) mice (Fig. 1f), where *ATR*-null cells demonstrate no selective disadvantage over time²³. Consistent with previous studies²³, a rapid deterioration of the intestinal epithelium was observed in *ATR*^{mKO} mice 6 days after TAM treatment (Fig. 1e), reaching a nadir a few days later (7–14 days after TAM treatment, ref. 23). This degeneration coincided with a 28% mortality of *ATR*^{mKO} animals within 2 weeks of *ATR* deletion (Fig. 1a), after which time compensatory tissue renewal from residual *ATR*-expressing progenitors allowed *ATR*^{mKO} mice to survive similar to controls for up to one year²³.

Surprisingly, *p53* absence failed to prevent short-term mortality following *ATR* mosaic deletion and, in contrast, led to an accelerated and highly penetrant lethal phenotype, with greater than 94% of *p53*^{-/-}*ATR*^{mKO} mice dying within 2 weeks of TAM treatment at a median time of 8 days (Fig. 1a). The single surviving *p53*^{-/-}*ATR*^{mKO} mouse in these studies had an abnormally low deletion rate (60% brain deletion). However, this mouse exhibited hair-graying within one month of TAM treatment (Fig. 1b), a phenotype observed in

p53^{+/+}*ATR*^{mKO} mice only at significantly later time points (3–6 months)²³. Furthermore, histological analysis of mice sacrificed just prior to median mortality (6 days after TAM) revealed that *p53* absence failed to rescue acute bone marrow degeneration and exacerbated the acute deterioration of the intestinal epithelium observed in *ATR*^{mKO} mice (Fig 1c–e). Consistent with *ATR*'s essential role during DNA replication^{19–22}, decreased cellularity in the bone marrow was primarily attributable to loss of highly proliferative populations (myeloid) instead of largely quiescent subsets (T cells, Fig. 1d). Synthetic lethality and regenerative deficiencies were also observed in *p53*^{-/-}*ATR*^{mKO} mice under conditions of decreased TAM treatment and lower-than-average deletion rates (Fig. 1b and data not shown). These data indicate that *p53* deficiency fails to rescue acute bone marrow and intestinal degeneration seen in *ATR*^{mKO} mice and that *p53* is required for organismal survival following *ATR* deletion.

The multiple checkpoint defects conferred by *ATR* and *p53* loss (*ATR*, S/G2; *p53*, G1) might permit redundant S phase entry and additive genome destabilization. Indeed, a synthetic-lethal interaction between *ATR-Chk1* pathway inhibition and *p53* deficiency is observed in cultured cells (ref. 24–26 and data not shown). However, accelerated depletion of *ATR*-deleted cells did not appear to be the primary cause of tissue failure in *p53*^{-/-}*ATR*^{mKO} mice, as *ATR*^{-/-} cells were represented at similar or higher frequencies in the intestines and bone marrow in comparison to *ATR*^{mKO} mice (Fig. 1f). In addition, mitotic spreads from freshly isolated *p53*^{-/-}*ATR*^{mKO} bone marrow exhibited mild and extensive chromatid breaks at an elevated frequency and significantly increased severity (Supplementary Fig. 2). Such levels of genomic instability in the absence of exogenous DNA-damaging treatments are hallmarks of *ATR* deletion^{19–22}. Together, these data argue that tissue homeostasis in *p53*^{-/-}*ATR*^{mKO} mice is compromised despite the continued maintenance of *ATR*^{-/-} cells.

ATR deletion leads to dramatic increases in genomic instability during DNA synthesis, resulting in H2AX phosphorylation (γ H2AX)^{20,21}. Notably, the frequency of cells exhibiting H2AX phosphorylation in the bone marrow and intestines of *p53*^{-/-}*ATR*^{mKO} mice was dramatically increased compared to *ATR*^{mKO} controls (Fig. 2). γ H2AX staining in the bone marrow was most prominent in cells with aberrantly large nuclei, which were morphologically distinguishable from multinucleated megakaryocytes or condensed apoptotic bodies (Fig. 2a). Indeed, *p53*-independent apoptosis (cleaved caspase-3 staining) was observed in minority fractions of γ H2AX-positive cells in both the bone marrow and intestines of *p53*^{-/-}*ATR*^{mKO} mice (Fig. 2c,f), leading to insignificant increases in total numbers of apoptotic cells (Supplementary Fig. 3c). Given that *ATR*^{-/-} cells were maintained at high levels in each of these tissues (Fig. 1f), these data are consistent with *p53* deficiency permitting the accumulation of *ATR*^{-/-} cells that have acquired DNA damage in the course of expansion.

Previous studies have indicated that tissue maintenance in *ATR*^{mKO} mice following acute deletion is dependent on compensatory renewal from cells that have escaped lox recombination and continue to express *ATR*²³. We sought to directly investigate whether the increased abundance of DNA-damaged cells in *p53*^{-/-}*ATR*^{mKO} mice detrimentally affects this regenerative response. To both accurately monitor the process of regeneration

and circumvent the lethality associated with systemic *ATR* and *p53* combined deletion, we studied the effect of localized *ATR* deletion on depilation-induced hair follicle regeneration in the skin. Localized *ATR* deletion was accomplished through topical treatment with 4-hydroxytamoxifen (4-OHT). Four days after cessation of 4-OHT treatment, hair follicle regeneration was synchronously induced by telogen-phase depilation (plucking) of the hair shafts in the central portion of a larger 4-OHT treatment (*ATR*-deleted) region.

As previously described, only a short delay in hair regeneration (3–4 days) was observed in *ATR^{mKO}* skin in comparison to *ATR^{mHet}* controls following a single round of depilation (ref. 23 and data not shown). In sharp contrast, hair regeneration in *p53^{-/-}ATR^{mKO}* skin was severely delayed compared to *ATR^{mKO}* skin, as indicated both by shaft regeneration (Fig. 3a) and formation of the hair follicle bulb (Fig. 3b). Closer examination of *p53^{-/-}ATR^{mKO}* skin revealed distinct malformations of the epithelium, root sheath and hair bulb, each of which was characterized by the presence of aberrant cells with enlarged nuclei (Fig. 3b). Notably, following hair shaft regeneration, an increased abundance of gray hair was observed in *p53^{-/-}ATR^{mKO}* skin both in the depilated region and the surrounding *ATR*-deleted region (Fig. 3c); this increase far exceeded that observed after a single round of depilation in *ATR^{mKO}* skin (Fig. 3a and ref. 23). These results indicate that combined loss of *ATR* and *p53* dramatically impedes hair follicle renewal and leads to long-term deficiencies in regenerated hair shafts (hair graying).

The short-term regenerative defect observed in *p53^{-/-}ATR^{mKO}* skin was accompanied by a severe inflammatory response, as characterized by reddening, exfoliation, and the recruitment of Gr1⁺Mac1⁺ innate immune cells (Fig. 3a,d). Inflammation initially occurred at the site of depilation and spread outwardly to eventually cover the entire *ATR*-deleted region (Fig. 3a). This phenotype was not observed in *ATR^{mKO}* or *ATR^{mHet}* controls (Fig. 3a,d and ref. 23). To determine whether delayed follicle regeneration in *p53^{-/-}ATR^{mKO}* skin was a consequence of acute inflammation, the topical immunosuppressant dexamethasone (dex) was applied 4 days after depilation and subsequently. This treatment was sufficient to prevent skin reddening and inhibit Gr1⁺Mac1⁺ innate immune cell infiltration into *p53^{-/-}ATR^{mKO}* epithelium and did not affect hair follicle generation in controls (Fig. 3d and Supplementary Fig. 4). However, dex treatment did not rescue hair follicle regeneration in *p53^{-/-}ATR^{mKO}* skin (Fig. 3e and Supplementary Fig. 4). Interestingly, cessation of dex treatment 22 days after depilation in *p53^{-/-}ATR^{mKO}* skin was immediately followed by a severe inflammatory response (Supplementary Fig. 4), indicating that the cause of inflammation in *p53^{-/-}ATR^{mKO}* skin continued to be present in the tissue for up to 3 weeks after depilation. In summary, while it is possible that innate immune infiltration and the gross pathological effects of inflammation in *p53^{-/-}ATR^{mKO}* skins may ultimately impact tissue maintenance in some manner (e.g. hair graying), they do not appear to be the primary cause of short-term delays in hair follicle regeneration.

To assess original *ATR* deletion rates prior to depilation (telogen phase) and quantify the representation of *ATR* cells during follicle regeneration, the recombination status of the *ATR^{fllox}* allele was determined both before (Day 0) and 4 and 8 days after depilation. The frequencies of *ATR* cells (either *ATR^{+/+}* or *ATR^{-/-}*) were similar in all genotypes both prior to depilation (Day 0) and in early anagen phase (4 days after depilation, Fig. 4a). These

results indicate that deletion rates (approximating 90% in the epithelium) were unaffected by *p53* status prior to depilation. While the frequencies of *ATR*^{-/-} cells were similar in early anagen, representation of these cells significantly decreased later in anagen (8 days after depilation) in both *ATR*^{mKO} and *p53*^{-/-}*ATR*^{mKO} skins (P = 0.0003, Fig. 4a). Similar to other tissues (Fig. 1f), this decline was not accentuated by *p53* deficiency (Fig. 4a), indicating that the regenerative delay in *p53*^{-/-}*ATR*^{mKO} skin occurred despite the continued maintenance of *ATR*^{-/-} cells.

We hypothesized that the regenerative defect in *p53*^{-/-}*ATR*^{mKO} skin may be caused by the persistent accumulation of highly damaged *ATR*^{-/-} cells, which would continue to occupy functional space and impede regeneration from residual *ATR*-expressing progenitors. To investigate this possibility, γ H2AX-positive cells were quantified in the general epithelium and in CD34⁺ α -6-integrin⁺ stem and progenitor cells, which are among the earliest populations of cells to proliferate and contribute to hair follicle renewal^{27–29}. In early anagen (day 4 post-depilation), the abundance of γ H2AX-positive cells was increased to similar extents in *ATR*^{mKO} and *p53*^{-/-}*ATR*^{mKO} skins, both in progenitor populations and in the general epithelium (Fig. 4b–d). Therefore, the generation of damaged *ATR*^{-/-} cells soon after exiting quiescence is not strongly influenced by *p53* function. However, at later stages of hair follicle regeneration (day 8 post-depilation), the frequency of γ H2AX-positive cells significantly declined in *ATR*^{mKO} skins and was maintained only in *p53*^{-/-}*ATR*^{mKO} skins (Fig. 4c,d). Interestingly, continued proliferation during differentiation from progenitors may amplify differences in the frequency of γ H2AX-positive cells between *ATR*^{mKO} and *p53*^{-/-}*ATR*^{mKO} skins (Fig. 4c,d). γ H2AX-positive cells exhibited enlarged nuclei that were morphologically distinct from apoptotic cells, consistent with the low frequency of cells staining positive for cleaved caspase-3 (Supplementary Fig. 5). These data indicate that *ATR* deletion in the absence of *p53* leads to the persistent accumulation of genetically unstable *ATR*^{-/-} cells.

We then examined whether the accrual of γ H2AX-positive cells in *p53*^{-/-}*ATR*^{mKO} skin was associated with defective compensatory renewal from residual cells that escaped *ATR* deletion. Consistent with previous studies²³, a large fraction of *ATR*^{mKO} hair follicles began to develop hair bulbs within 8 days of depilation (Fig. 5). These bulbs exhibited cellular proliferation (nuclear PCNA staining) and were largely comprised of cells that expressed the *ATR*/*ATRIP* complex (Fig. 5). In contrast, *p53*^{-/-}*ATR*^{mKO} skin largely failed to undergo compensatory regeneration, as indicated by the absence of cellular proliferation in the hair bulb and the lack of expansion of *ATR*/*ATRIP*-positive cells (Fig. 5). These data indicate that the compensatory renewal driven by residual *ATR*-expressing cells is strongly impeded in *p53*^{-/-}*ATR*^{mKO} skin.

Previously, we have shown that *ATR*-deleted cells are rapidly eliminated from proliferative tissues and replaced through compensatory renewal by undeleted, *ATR*-expressing progenitors²³. The studies described herein demonstrate that *p53* limits the accumulation of highly damaged cells following mosaic *ATR*-deletion and argue that loss of this constraint delays tissue regeneration. These results strongly support the model that *p53* plays a key role in maintaining adult tissue homeostasis by preventing functionally compromised cells from acting as a barrier to progenitor-driven renewal^{15–18}. Occupancy of tissues with genetically

unstable cells might delay tissue renewal either by obstructing competent progenitors from interacting with key environmental cues or by causing the generation of secreted factors^{30,31} that inhibit renewal. Such mechanisms may operate as a tissue homeostatic checkpoint, delaying regeneration until damaged cells have been effectively cleared.

The degeneration of tissue integrity following combined loss of *ATR* and *p53* is somewhat unexpected given that *p53* deficiency generally attenuates the effects of mutations in other genome maintenance regulators^{1–12}. While *p53* loss may be sufficient to accommodate lesser degrees of genomic instability and permit mildly damaged cells to functionally contribute to tissue homeostasis, it is likely that the severe cell cycle and genome destabilizing consequences of *ATR* deficiency are not alleviated by *p53*'s absence and, rather, are exacerbated by it. According to this model, replication fork instability in concert with near-complete loss of cell cycle checkpoint functions without *ATR* and *p53* might allow redundant or aberrant S phase entry, leading to further instability and the inappropriate propagation of terminally damaged cells. Indeed, the persistent accumulation of genetically unstable cells in *p53*^{-/-}*ATR*^{mKO} tissues compared to *p53* wild-type *ATR*^{mKO} controls supports this model (Fig. 2, Fig. 4c,d and Supplementary Fig. 2). Therefore, in addition to supporting a general function for *p53* in facilitating regeneration of adult tissues, this study provides the first evidence of a specific synthetic interaction between *ATR* and *p53* inhibition in adult mammals. These results suggest that *ATR*-*Chk1* inhibitors may be uniquely useful for the treatment of *p53*-deficient cancers by causing synergistic increases in genomic instability, which may consequentially inhibit regeneration from undamaged bystanders.

METHODS

Methods and associated references are available in the online version of the paper at <http://www.nature.com/naturegenetics/>.

Supplementary Material

Refer to Web version on PubMed Central for supplementary material.

ACKNOWLEDGMENTS

We are indebted to Gregory Beatty, Karlene Cimprich, George Cotsarelis and Avinash Bhandoola for reagents, protocols and helpful advice and the AFCRI Histology Core for tissue processing. These studies were supported by the National Institute on Aging (R01AG027376 and F30AG034027) and the Abramson Family Cancer Research Institute.

REFERENCES

1. Wlodarski P, et al. Role of *p53* in hematopoietic recovery after cytotoxic treatment. *Blood*. 1998; 91:2998–3006. [PubMed: 9531612]
2. Bender CF, et al. Cancer predisposition and hematopoietic failure in *Rad50*(S/S) mice. *Genes Dev*. 2002; 16:2237–2251. [PubMed: 12208847]
3. Chin L, et al. *p53* deficiency rescues the adverse effects of telomere loss and cooperates with telomere dysfunction to accelerate carcinogenesis. *Cell*. 1999; 97:527–538. [PubMed: 10338216]

4. Frank KM, et al. DNA ligase IV deficiency in mice leads to defective neurogenesis and embryonic lethality via the p53 pathway. *Mol Cell*. 2000; 5:993–1002. [PubMed: 10911993]
5. Gao Y, et al. Interplay of p53 and DNA-repair protein XRCC4 in tumorigenesis, genomic stability and development. *Nature*. 2000; 404:897–900. [PubMed: 10786799]
6. Hakem R, de la Pompa JL, Elia A, Potterx J, Mak TW. Partial rescue of Brca1 (5–6) early embryonic lethality by p53 or p21 null mutation. *Nat Genet*. 1997; 16:298–302. [PubMed: 9207798]
7. Lim DS, Hasty P. A mutation in mouse rad51 results in an early embryonic lethal that is suppressed by a mutation in p53. *Mol Cell Biol*. 1996; 16:7133–7143. [PubMed: 8943369]
8. Lim DS, et al. Analysis of ku80-mutant mice and cells with deficient levels of p53. *Mol Cell Biol*. 2000; 20:3772–3780. [PubMed: 10805721]
9. Xu Y, Yang EM, Brugarolas J, Jacks T, Baltimore D. Involvement of p53 and p21 in cellular defects and tumorigenesis in *Atm*^{-/-} mice. *Mol Cell Biol*. 1998; 18:4385–4390. [PubMed: 9632822]
10. Xu X, et al. Genetic interactions between tumor suppressors Brca1 and p53 in apoptosis, cell cycle and tumorigenesis. *Nat Genet*. 2001; 28:266–271. [PubMed: 11431698]
11. Botchkarev VA, et al. p53 is essential for chemotherapy-induced hair loss. *Cancer Res*. 2000; 60:5002–5006. [PubMed: 11016618]
12. Orii KE, Lee Y, Kondo N, McKinnon PJ. Selective utilization of nonhomologous end-joining and homologous recombination DNA repair pathways during nervous system development. *Proc Natl Acad Sci U S A*. 2006; 103:10017–10022. [PubMed: 16777961]
13. Tyner SD, et al. p53 mutant mice that display early ageing-associated phenotypes. *Nature*. 2002; 415:45–53. [PubMed: 11780111]
14. Maier B, et al. Modulation of mammalian life span by the short isoform of p53. *Genes Dev*. 2004; 18:306–319. [PubMed: 14871929]
15. Matheu A, et al. Delayed ageing through damage protection by the Arf/p53 pathway. *Nature*. 2007; 448:375–379. [PubMed: 17637672]
16. Serrano M, Blasco MA. Cancer and ageing: convergent and divergent mechanisms. *Nat Rev Mol Cell Biol*. 2007; 8:715–722. [PubMed: 17717516]
17. Garcia-Cao I, et al. Increased p53 activity does not accelerate telomere-driven ageing. *EMBO Rep*. 2006; 7:546–552. [PubMed: 16582880]
18. Krizhanovsky V, et al. Senescence of activated stellate cells limits liver fibrosis. *Cell*. 2008; 134:657–667. [PubMed: 18724938]
19. Brown EJ, Baltimore D. ATR disruption leads to chromosomal fragmentation and early embryonic lethality. *Genes Dev*. 2000; 14:397–402. [PubMed: 10691732]
20. Brown EJ, Baltimore D. Essential and dispensable roles of ATR in cell cycle arrest and genome maintenance. *Genes Dev*. 2003; 17:615–628. [PubMed: 12629044]
21. Chanoux RA, et al. ATR and H2AX Cooperate in Maintaining Genome Stability under Replication Stress. *J Biol Chem*. 2009; 284:5994–6003. [PubMed: 19049966]
22. Paulsen RD, Cimprich KA. The ATR pathway: fine-tuning the fork. *DNA Repair (Amst)*. 2007; 6:953–966. [PubMed: 17531546]
23. Ruzankina Y, et al. Deletion of the developmentally essential gene ATR in adult mice leads to age-related phenotypes and stem cell loss. *Cell Stem Cell*. 2007; 1:113–126. [PubMed: 18371340]
24. Zhou BB, Bartek J. Targeting the checkpoint kinases: chemosensitization versus chemoprotection. *Nat Rev Cancer*. 2004; 4:216–225. [PubMed: 14993903]
25. Nghiem P, Park PK, Kim Y, Vaziri C, Schreiber SL. ATR inhibition selectively sensitizes G1 checkpoint-deficient cells to lethal premature chromatin condensation. *Proc Natl Acad Sci U S A*. 2001; 98:9092–9097. [PubMed: 11481475]
26. Nghiem P, Park PK, Kim Ys YS, Desai BN, Schreiber SL. ATR is not required for p53 activation but synergizes with p53 in the replication checkpoint. *J Biol Chem*. 2002; 277:4428–4434. [PubMed: 11711532]
27. Morris RJ, et al. Capturing and profiling adult hair follicle stem cells. *Nat Biotechnol*. 2004; 22:411–417. [PubMed: 15024388]
28. Greco V, et al. A two-step mechanism for stem cell activation during hair regeneration. *Cell Stem Cell*. 2009; 4:155–169. [PubMed: 19200804]

29. Blanpain C, Lowry WE, Geoghegan A, Polak L, Fuchs E. Self-renewal, multipotency, and the existence of two cell populations within an epithelial stem cell niche. *Cell*. 2004; 118:635–648. [PubMed: 15339667]
30. Coppe JP, et al. Senescence-associated secretory phenotypes reveal cell-nonautonomous functions of oncogenic RAS and the p53 tumor suppressor. *PLoS Biol*. 2008; 6:2853–2868. [PubMed: 19053174]
31. Kuilman T, Peeper DS. Senescence-messaging secretome: SMS-ing cellular stress. *Nat Rev Cancer*. 2009; 9:81–94. [PubMed: 19132009]
32. Cortez D, Guntuku S, Qin J, Elledge SJ. ATR and ATRIP: partners in checkpoint signaling. *Science*. 2001; 294:1713–1716. [PubMed: 11721054]

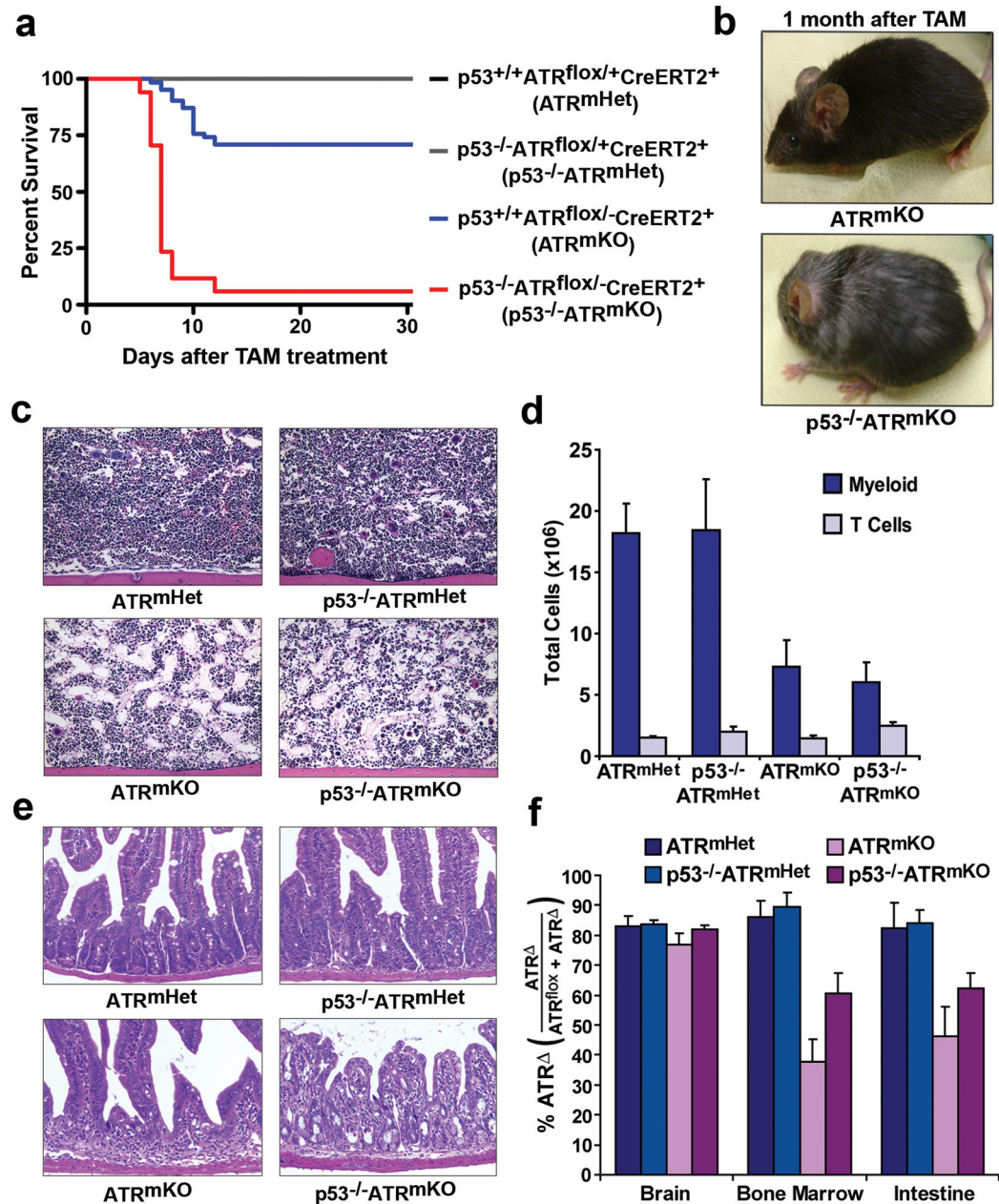


Figure 1.

Mosaic *ATR* deletion in adult mice is synthetic lethal with *p53* deficiency. (a) Kaplan-Meier representation of survival following acute, mosaic *ATR* deletion in $p53^{+/+}$ and $p53^{-/-}$ mice. Approximately 72% of ATR^{mKO} mice survive the immediate period following TAM treatment, while less than 6% of $p53^{-/-}ATR^{mKO}$ mice (1 in 17) were viable beyond this time. (b) The single surviving $p53^{-/-}ATR^{mKO}$ mouse (from part a) and a comparably treated ATR^{mKO} mouse 1 month after TAM treatment. (c) H&E stained sections of the humeral bone from mice of the indicated genotypes 6 days after TAM treatment, 200 \times ;

magnification. **(d)** Absolute number of myeloid cells (Gr1⁺) and T cells (CD3, CD4, or CD8⁺) obtained from 4 hindlimb bones 6 days after TAM treatment ($n = 4-5$ mice per genotype). The loss of myeloid cells from the bone marrow of ATR^{mKO} and $p53^{-/-}ATR^{mKO}$ relative to each respective $ATR^{lox/+}$ control was significant ($P = 0.01$ and 0.03 , respectively). **(e)** H&E stained sections of intestines from mice of the indicated genotypes 6 days after TAM treatment, 200 \times magnification. **(f)** Abundance of the ATR^{lox} -recombined allele (ATR) in the brain, bone marrow, and intestines 6 days after TAM treatment ($n = 7-12$ mice per genotype). The frequency of ATR^{lox} recombination was determined by quantitative PCR amplification of the ATR^{lox} allele from genomic DNA isolated from each tissue (described in *Methods*). P values from *t tests* comparing the mean frequencies of ATR in $p53^{-/-}ATR^{mKO}$ and ATR^{mKO} mice were 0.047 and 0.149 in the bone marrow and intestines, respectively. Error bars in both **d** and **f** represent the S.E.M. of each data set.

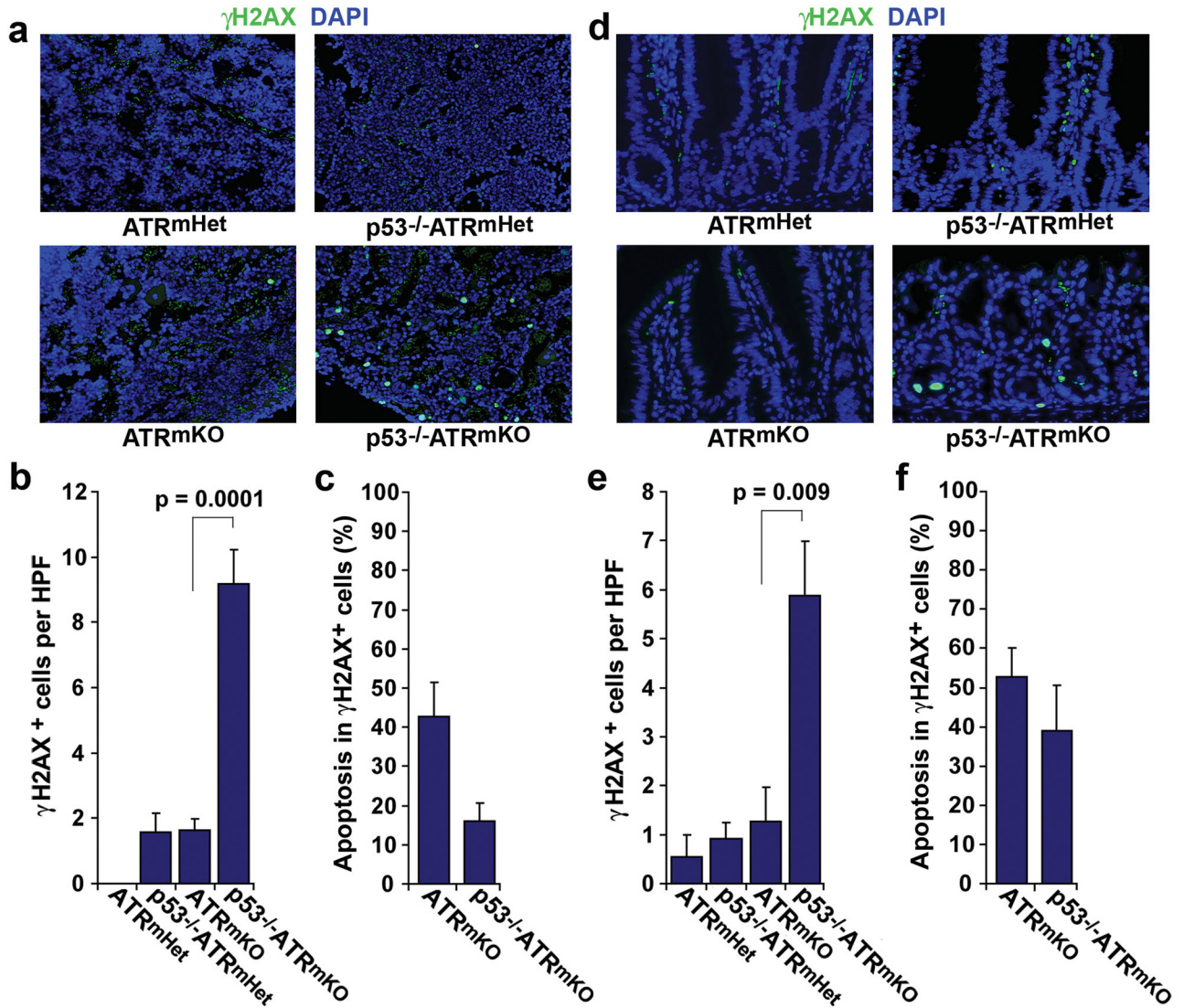


Figure 2. Accumulation of damaged cells in the bone marrow and intestines of *p53^{-/-}ATR^{mKO}* mice. (a) Representative γ H2AX (green) and DAPI (blue) stained sections of the humeral bones from mice of the indicated genotypes 6 days after TAM treatment. Autofluorescent red blood cells (green, DAPI negative) in the sinusoidal spaces of the marrow were excluded from further analysis. (b) Quantification of γ H2AX-positive cells in the bone marrow. The abundance of γ H2AX-positive cells was determined from 6–10 high power field images (HPF, 200 \times) of indicated mice ($n = 3$ –6 mice per genotype). Only nucleated (DAPI-positive) cells were scored in this analysis. (c) Frequency of γ H2AX-positive cells staining positive for cleaved caspase-3, as determined by co-immunostaining (also see Supplementary Fig. 3a). (d) Representative γ H2AX (green) and DAPI (blue) stained intestinal sections from mice of the indicated genotypes 6 days after TAM treatment. Autofluorescent red blood cells (green, DAPI negative) in the vasculature and stroma were

excluded from quantifications. **(e)** Quantification of γ H2AX-positive cells in intestinal epithelium ($n = 2-6$ mice per genotype). The abundance of γ H2AX-positive cells was determined as in **b**. **(f)** Frequency of γ H2AX-positive cells staining positive for cleaved caspase-3, as determined by co-immunostaining (also see Supplementary Fig. 3b). Error bars in **b**, **c**, **e** and **f** represent the S.E.M. of each data set.

Author Manuscript

Author Manuscript

Author Manuscript

Author Manuscript

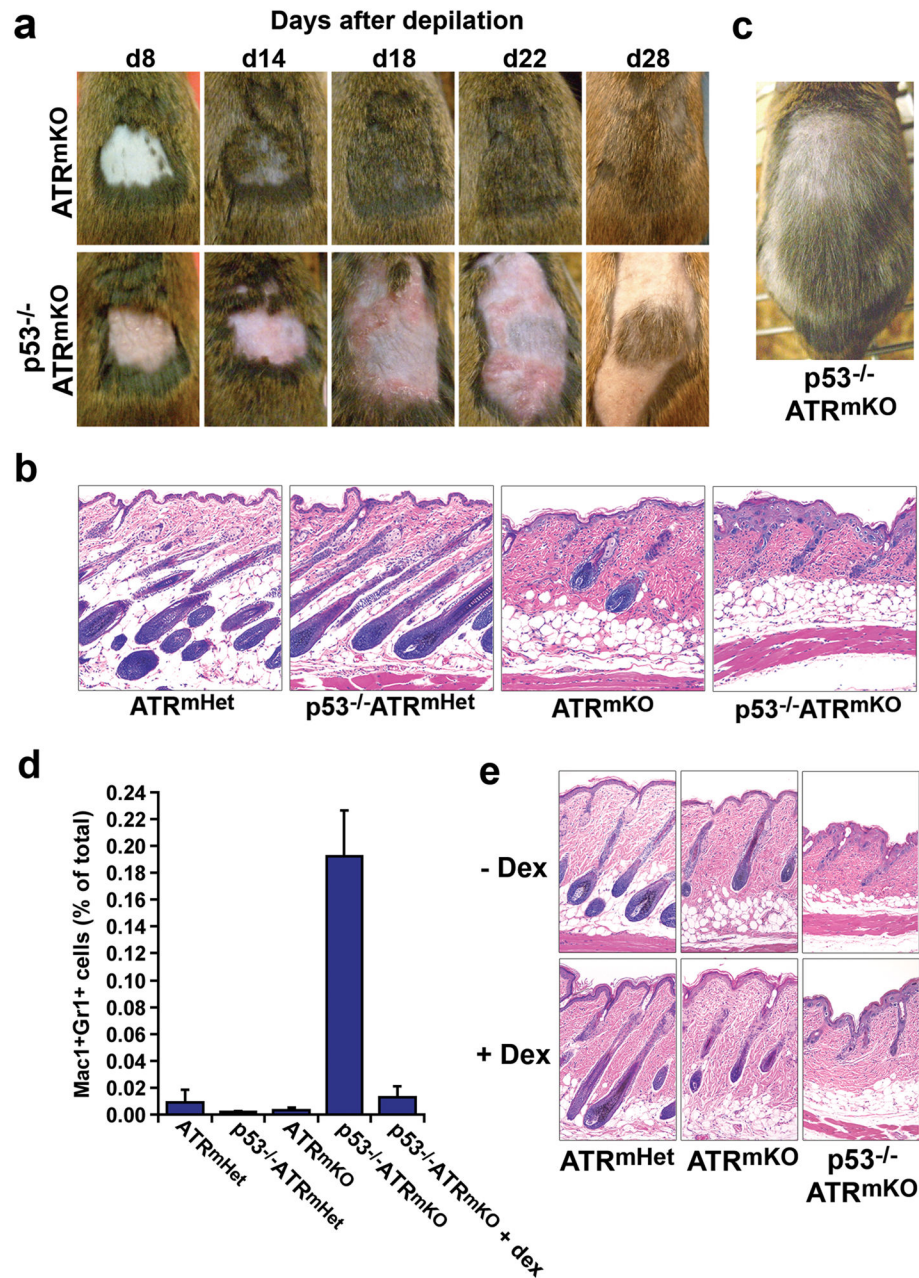


Figure 3. *p53* deficiency dramatically delays hair follicle regeneration following localized *ATR* deletion in the skin and leads to acute inflammation. **(a)** Time course following depilation of 4-OHT-treated skins of *ATR*^{lox/-} and *p53*^{-/-}*ATR*^{lox/-} mice. An appreciable delay in hair regeneration after depilation was observed in *p53*^{-/-}*ATR*^{mKO} skin and was accompanied by the outward manifestations of inflammation (redness, swelling, exfoliation). These phenotypes were consistently observed in *p53*^{-/-}*ATR*^{mKO} mice ($n = 6-12$ mice per genotype). **(b)** Representative H&E stained sections of the epidermis 8 days after depilation.

The number and quality of regenerating follicles were compromised in the $p53^{-/-}ATR^{mKO}$ skin relative to ATR^{mKO} or $ATR^{lox/+}$ control skins ($n = 5-7$ mice per genotype). **(c)** Regenerated hair in $p53^{-/-}ATR^{mKO}$ skin 48 days after depilation. Appreciable hair graying was observed in $p53^{-/-}ATR^{mKO}$ skin in the depilated and surrounding 4-OHT treatment regions ($n = 6$ mice). **(d)** Quantification of $Gr1^{+}Mac1^{+}$ inflammatory cells in the epidermis 8 days after depilation ($n = 4-5$ mice per genotype). Total epidermal cells were isolated (*Methods*), stained with antibodies to Gr1 and Mac1 (CD11b), and the frequency of $Gr1^{+}Mac1^{+}$ cells was quantified by flow cytometry. $Gr1^{+}Mac1^{+}$ cells accumulated significantly in $p53^{-/-}ATR^{mKO}$ skin ($P = 3 \times 10^{-7}$), and dexamethasone pretreatment of $p53^{-/-}ATR^{mKO}$ skin (+ dex) prevented $Gr1^{+}Mac1^{+}$ cell accumulation, $P = 0.003$. Error bars, s.e.m. **(e)** H&E stained sections of skin 8 days after depilation in the presence or absence of dex. Mice treated with dex or left untreated were sacrificed 8 days after depilation. Delayed follicle regeneration in $p53^{-/-}ATR^{mKO}$ skin was unaffected by dexamethasone treatment ($n = 4$ mice per genotype).

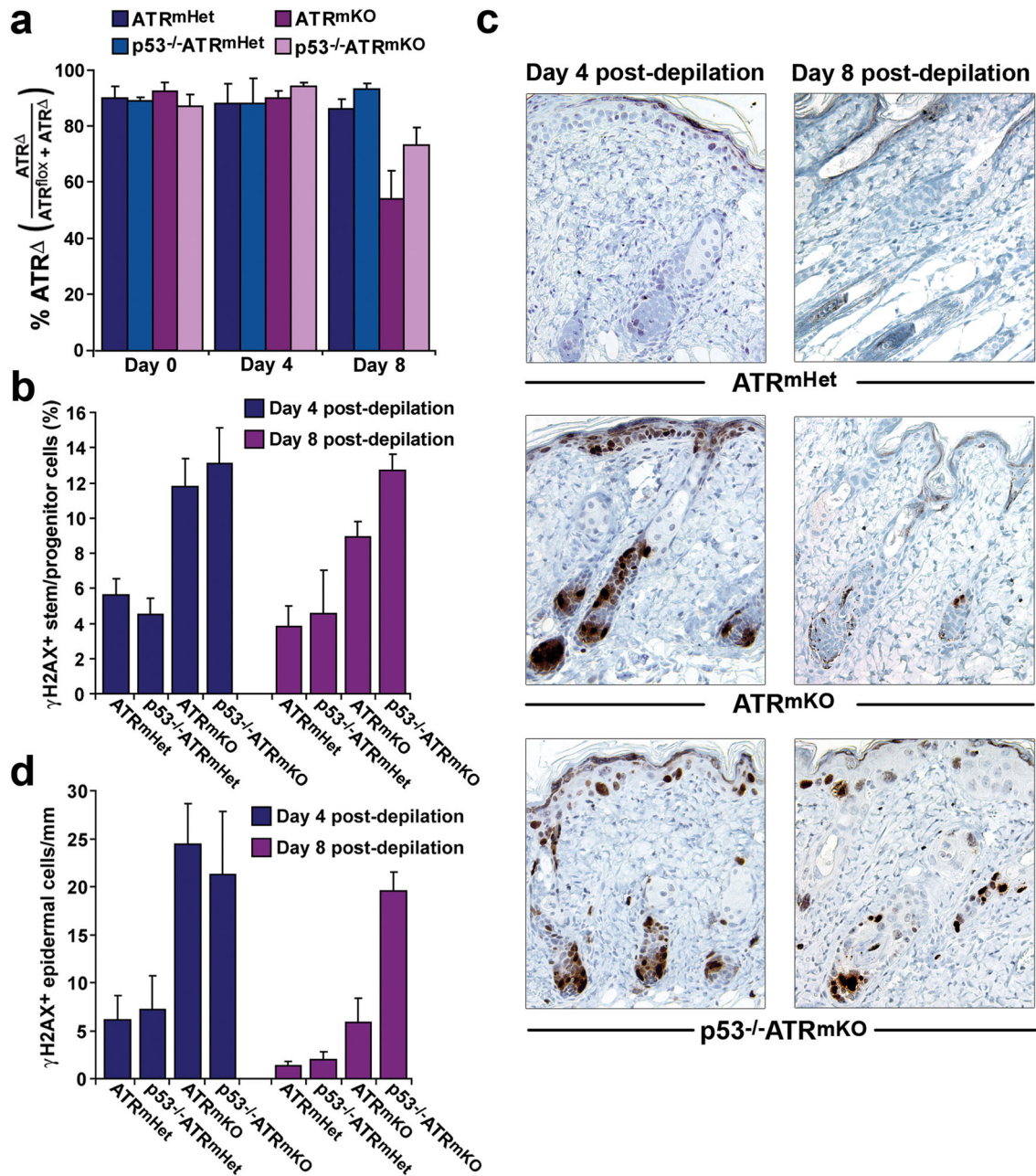


Figure 4. *p53^{-/-}ATR^{mKO}* skin is characterized by the persistent accumulation of γ H2AX-positive cells. (a) Frequency of the *ATR^{flox}*-recombined allele (*ATR^Δ*) in epidermal isolates at different time points after depilation ($n = 3-13$ mice per genotype per time point). Recombination of the *ATR^{flox}* allele was quantified by qPCR amplification of genomic DNA isolated from total epidermal cells (described in *Methods*). (b) Frequency of γ H2AX-positive epidermal stem and progenitor cells ($CD34^+\alpha$ -6-integrin⁺) isolated from skin 4 days and 8 days following depilation. The difference in mean abundance of γ H2AX-positive cells

between $p53^{-/-}ATR^{mKO}$ and ATR^{mKO} skins 8 days post-depilation was significant ($P = 0.023$). (c) Representative γ H2AX (brown) and hematoxylin (blue) stained sections of the skin 4 days and 8 days after depilation. (d) Quantification of γ H2AX-positive cells in the hair follicles and epidermis of depilated skin. Frequency of γ H2AX-positive cells was determined in 6–10 sections per mouse ($n=3-5$ mice per genotype for each time point). Note the elevated frequency of γ H2AX-positive cells in both ATR^{mKO} and $p53^{-/-}ATR^{mKO}$ skins 4 days post-depilation; however, this significant increase was maintained only in $p53^{-/-}ATR^{mKO}$ skin 4 days later (day 8 post-depilation). The difference in mean abundance of γ H2AX-positive cells between $p53^{-/-}ATR^{mKO}$ and ATR^{mKO} skins 8 days post-depilation was significant ($P = 0.013$). Increased frequency of γ H2AX-positive cells in $p53^{-/-}ATR^{mKO}$ skin was observed both in the presence and absence of dexamethasone (Supplementary Fig. 4).

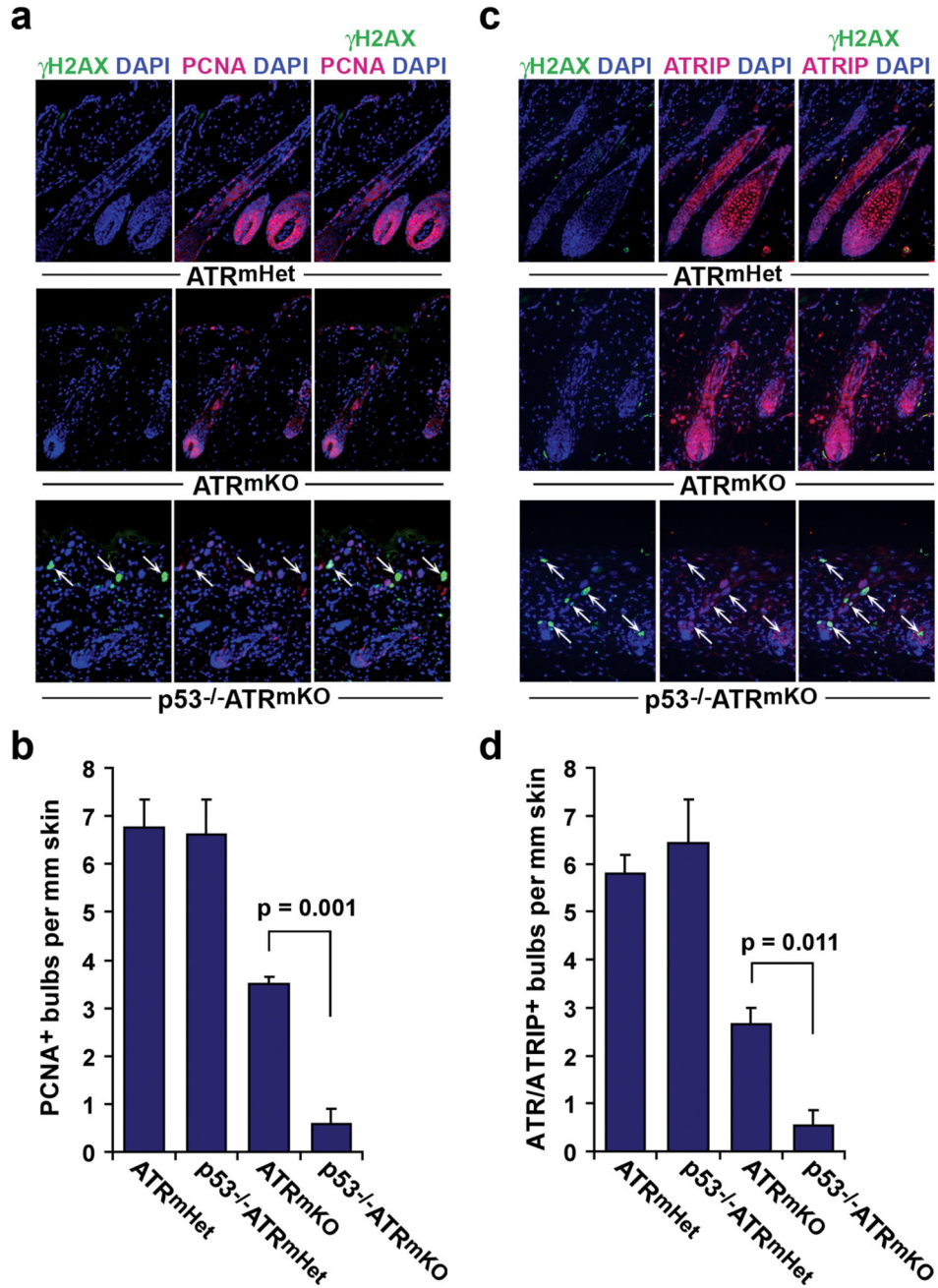


Figure 5.

p53 is required for efficient compensatory renewal following *ATR* deletion. (a) Representative PCNA (red), γ H2AX (green), and DAPI (blue) stained sections of skin 8 days after depilation. γ H2AX-positive cells are indicated (white arrows). (b) Quantification of regenerating PCNA-positive bulbs per mm skin. (c) Follicle regeneration in *ATR*^{mKO} skin by ATR/ATRIP-expressing cells. Representative ATRIP (red), γ H2AX (green), and DAPI (blue) stained sections of skin 8 days after depilation. ATR and ATRIP form an interdependent complex in which ATR is required for ATRIP stability³². γ H2AX-positive

cells are indicated (white arrows). **(d)** Quantification of ATR/ATRIP-expressing bulbs per mm skin. Analyses and quantifications for **b** and **d** were performed on 6–12 sections per mouse ($n=3$ mice per genotype). Error bars represent S.E.M. for each data set.